LA-UR- 08-6471

Approved for public release; distribution is unlimited.

Title:	High-temporal contrast using low-gain optical parametric amplification
Author(s):	Rahul C. Shah, Randall P. Johnson, Tsutomu Shimada, Kirk A. Flippo, Juan C. Fernandez, and B. M. Hegelich
Intended for:	Optics Letters

Form 836 (7/06)

Author List Continued (Shah, Form 678)

Last	First	Middle	Z No.	Group
Fernandez	Juan	C.	098757	P-24
Hegelich	Bjorn	M.	186672	P-24

High-temporal contrast using low-gain optical parametric amplification

Rahul C. Shah, Randall P. Johnson*, Tsutomu Shimada, Kirk A. Flippo, Juan C. Fernandez, and, B. M. Hegelich

Los Alamos National Laboratory, Los Alamos, NM 87545 USA,
**Corresponding author: rpjohnson@lanl.gov*

Compiled September 19, 2008

We demonstrate the use of low-gain optical parametric amplification (OPA) as a means of improving temporal contrast. 250 μJ, 500 fs pulses of 1053 nm are frequency doubled and subsequently restored to original wavelength by the OPA with > 10% efficiency.

OCIS codes: 190.4970, 230.4480, 170.7160, 140.3538

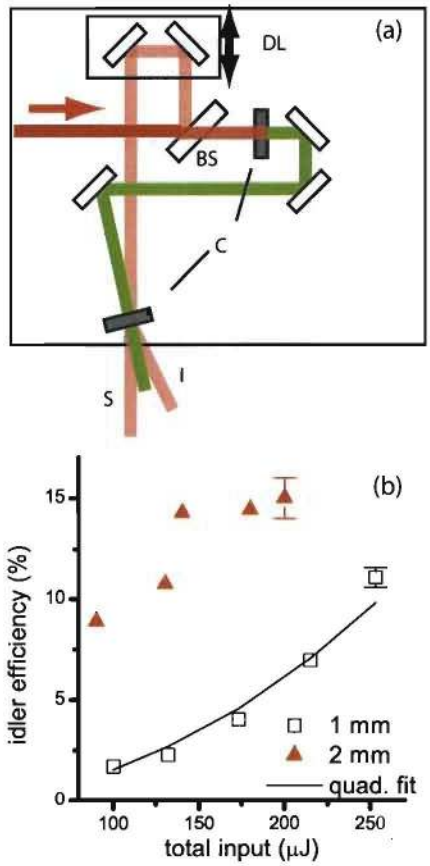

Fig. 1. (a) Schematic of low gain OPA temporal pulse cleaning: DL, delay line; BS, 10/90 beamsplitter; C, 2 mm Type I BBO crystal; S, signal; and I, idler. (b) Idler efficiency for both 1 and 2 mm crystals. shahFIG1.eps.

Realization of promising applications of relativistic light intensities achieved with terawatt chirped pulse amplification (CPA) lasers [1] depends on the ability to control premature target ionization by preceding intensity spikes, compression quality, or amplified spontaneous emission (ASE). As an example, the threshold for destruction of ~nm target foils in laser-based ion acceleration schemes [2] occurs at 10^{10} W/cm^2. At typical peak interaction intensities of 10^{20} W/cm^2, this translates to a requirement of better than 10^{-10} intensity contrast a few ps from the peak. Given the absolute damage threshold, as laser intensities continue to grow [3], so to will the contrast requirement. This short timescale dictates the use of non-linear optical processes to remove the ASE.

Since the strength of the ASE depends on the total gain it sees, temporal cleaning subsequent to initial gain stages suffices to reduce its level to the contrast criteria. Most current systems then require temporally clean pulses of 10s of μJ though the exact requirement depends on the pulse duration and final energy. Such clean pulse energies can be obtained by first amplifying a temporally stretched pulse and then compressing it for cleaning with a non-linear technique. Before subsequent amplification, the pulse passes through another stretcher. Demonstration of this scheme, called double-CPA, showed the ASE reduced to at least 10^{-10} at up to 25 ps before the pulse-peak [4]. In future higher power systems, the ASE considerations will increase the necessary clean pulse energy.

Temporal cleaning using third-order non-linear optics (χ^3) requires an intensity of order 10^{11}-10^{12}W/cm^2. In the case of a crystal for cross-polarization-wave generation [5], pulses > 1 ps exceed the fluence damage at this intensity . Access of χ^3 effects also brings about self-focusing effects which may degrade beam quality in near-field application.

OPA, a second-order non-linear process (χ^2) in which a pump wave amplifies a lower frequency signal, offers an alternative using order GW/cm^2. Optical parametric noise (OPN) generates an incoherent background analogous to ASE with the distinction that its temporal duration matches that of the pump. Using a pump laser of <10 ps duration windowed the amplification of the ~ps input to maintain high contrast [6]. In addition to amplification of a signal wave, OPA generates a third wave, referred to as the idler. Most recently high gain OPA with chirp compensation generated ultra-broad bandwidth idler for which the combination of pump duration and chirp imply OPN window <1 ps [7].

In this letter we show that idler generation from low gain OPA, provides an insertable approach for improv-

ing temporal contrast. Working in the near-field, 250 μJ, 500 fs pulses of 1053 nm are frequency doubled and subsequently restored to original wavelength by the OPA with >10% efficiency. Low gain (2-20x) allows thinner crystals and minimizes bandwidth loss due to energy velocity mismatch. The results agree with expected temporal cubing of the input signal , show stability on par with that of the input, and preserve spectral width and spatial quality.

The cubic relationship between the temporal profile of the idler and signal becomes apparent from analytical OPA solution neglecting pump depletion with low gain. Let I_i, I_s, I_p refer to the idler, signal and pump intensities respectively. For $gz/2 < 1$ where z refers to propagation length and $g \propto \sqrt{I_{p0}}$, one finds $I_i \approx I_{s0}(gz/2)^2$. The cubic dependence occurs if the pump forms by doubling a portion of the original signal giving $I_p \propto {I_s}^2$. The non-linear restoration of the original wavelength improves the temporal contrast *beyond* that of the initial up-conversion. Even with larger gain, the exponential gain of the pump will fall into this cubic approximation in the temporal wings. The same holds for saturation effects. From Manley-Rowe, the idler energy matches that added to the signal pulse. Assuming 50% doubling efficiency due to Gaussian beam profile, picking off 10% of the initial energy as signal corresponds to an unsaturated gain of ~3 for complete pump extraction. For Type I phase matching, a slightly non-collinear geometry allows separation of the signal and idler. Using high quality surfaces, free propagation and a well-collimated beam minimizes scatter from the signal which would degrade the contrast.

Fig. 1(a) presents the low-gain OPA pulse cleaning scheme more clearly. In the final version, a 90/10 beamsplitter divides near-transform limit 1053 nm, 500 fs pulses of up to 250 μJ. The larger portion doubles by passing through 2 mm, Type I BBO with maximum efficiency near 70%. The s-polarized 527 nm light and the seed fundamental light then mix at $\sim 4°$ in an identical BBO crystal for which an adjustable delay in the infra-red path allows temporal superposition. The 3 mm input beam diameter satisfies the geometric constraint imposed by pulse duration and separation angle. With I_p ~4 GW/cm^2, the unsaturated gain measures 11. To demonstrate the scaling in the un-saturated regime, data using a 1 mm crystal, cut for larger angle mixing, is also presented. In that case, the pulses were only compressed to $\sim$ 2 ps and the mixing occurred at $\sim 10°$ with converging beams at diameter ~1 mm.

The scaling data are presented in Fig. 1(b) with representative measurement error bars. For the thinner crystal the measured efficiency fits a quadratic scaling for all data points with gain<2. For a cubic process the shot-to-shot stability scales as 3x that of input. In the case of the 2 mm crystal, the efficiency curve evidences strong saturation which results in 1:1 relative stability between input and output. For the latter, the extraction efficiency of the pump reaches 50% and overall efficiency 15%.

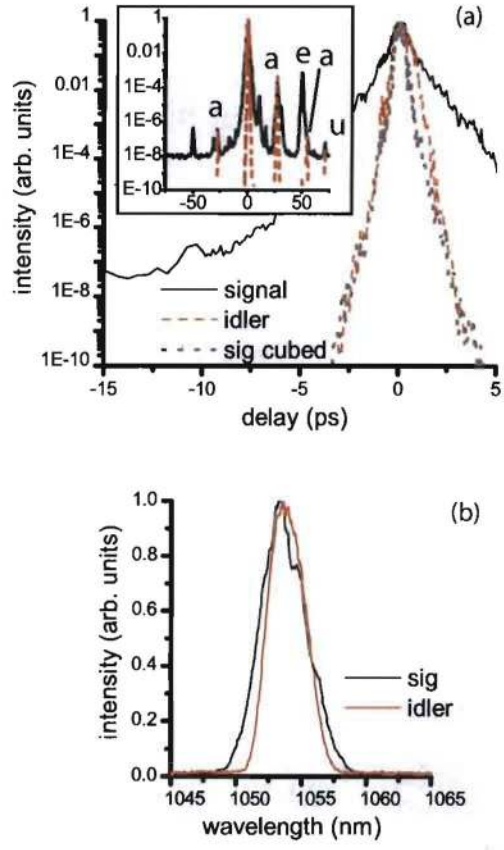

Fig. 2. (a) Temporal contrast measurement of both unamplified signal and idler with calculated cube of signal. Inset shows larger temporal range: a, known artifact; e, etalon reflection; u, unknown peak, presumed to be artifact. (b) Measured spectra. shahFIG2.eps.

A commercial third-order auto-correlator (Del Mar Photonics, San Diego) measured the temporal contrast with (idler) and without cleaning (signal with pump blocked) using ~30 μJ. As a fiducial, the beam passed a 5 mm etalon prior to the pulse cleaning setup. The inset of Fig. 2(a) presents a 150 ps window, representative of longer scans (1 ns maximum). The first order etalon reflection at 50 ps with intensity contrast 7×10^{-4} seen in the direct measure of the regenerative amplifier appears in the idler scan as a peak of 4×10^{-10}. There is remarkable agreement with the anticipated cubic relation from which one expects etalon peak of 3×10^{-10} in the cleaned pulse. As well, the ASE pedestal of contrast 10^{-8} and pre-pulse at -50 ps in the un-amplified signal fall below the near 10^{-10} detection limit of the device. In separate experiments we have measured scattering from signal beam to be of order 10^{-4} into $f/4$ collection at approximately the same separation angle [8]. Considering the diffraction limited divergence, the collected scattering would reduce by an additional 10^6. The net impact from scattering of a 10^{-3} reflection would then occur at

$< 10^{-13}$ and that of the ASE at 10^{-18}. Limitations of double-CPA would exceed these values. Several spikes occur identically in both cleaned and original pulses. Those labeled **a** correspond to first and second order reflections of the device filters. The origin of the postpulse of strength 6×10^{-8} at 71 ps has not been identified.

The central image of Fig. 2(a) shows a temporal zoom of the inset and also includes the cubed contrast of the signal. Corrections for saturation do not improve the fit of the cube: its impact is small with respect to the steepness of the fall-off. Though the temporal cubing implies a $\sqrt{3}$ reduction in duration, at the pulse peak, the durations appear equal. Saturation and/or group velocity mismatch (GVM) in the cleaning may cause this as calculated total slip of the fundamental and harmonic is 270 fs [9]. The largest deviation from the fit occurs between 0.2 and 2.5 ps. As each measurement took on the order of 30 minutes, known drift within the preceding stretcher and compressor can result in differing pulse shapes and durations. Several separate measurements supports this explanation.

The spectra of both signal and idler are shown in Fig. 2(b). Sharpening in the temporal domain (for example, cubing) corresponds to smoothing operations in frequency. Indeed, the discontinuities present in the signal spectrum are absent in the spectrum of the idler. The slight decrease (12%) in the spectral width brings the pulse closer to the transform limit. This could also mark a limit imposed by the afore mentioned GVM. Using partially compressed pulses (in the 1 mm crystal experiments) we have observed loss of bandwidth well matched by the theory presented for a χ^3 process [10]. We find optimal stability, width and spectral shape with slight manipulation of pulse chirp from that set by initial pulse duration measurements, presumably this optimizes compression in the mixing.

The final characterization essential for laser-chain implementation, that of near-field profile, is presented in Fig. 3. The beams directly fall upon the camera sensor at a distance $\sim$1 m from the mixing. Image (a) of input signal and (b) of idler clearly show that the OPA cleaning reduces the beam diameter, and the plotted lineouts (c) quantify the effect. Cubing of the input intensity (or steeper narrowing for larger gain) would occur both in time and space. Reduction by 1.5x indicates saturation only slightly fills the profile. This result then suggests that the temporal pulse-width stems primarily from GVM. Returning to Fig. 3, a second key point is the well-maintained quality of the near-field profile. At such low gains, some benefit may occur from the slight separation angle in the horizontal dimension as well as the Poynting walk-off in the vertical dimension which result in profile shearing on the order 160 and 100 μm respectively.

In summary we presented the use of low gain OPA as an insertable approach for temporal contrast improvement. The measured contrast improvement agrees well with expected temporal cubing, and we find better than

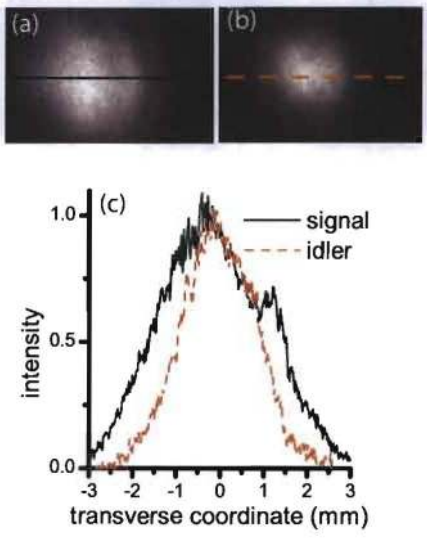

Fig. 3. Near-field spatial profile of (a) unamplified signal and (b) idler. shahFIG3.eps.

10% efficiency with 250 μJ input. Spectral width and quality have been preserved for the 500 fs pulses. Pulse tilting [11,12], or alternatively chirp compensation, could address both GVM limitations and geometric requirements of larger beam aperture. We hope that along with its current application within an intense-laser chain [13], our presented findings will also benefit future systems requiring high temporal contrast.

Authors acknowledge support of U.S. DOE and LANL Laboratory Directed Research and Development. R.S acknowledges assistance of Trident and P-24 staff.

References

1. M. D. Perry and G. Mourou, Sci. p. 917.
2. L. Yin, B. J. Albright, B. M. Hegelich, K. J. Bowers, K. A. Flippo, T. J. T. Kwan, and J. C. Fernández, Phys. Plasmas **14**, 056706 (2007).
3. E. Gerstner, Nat. **446**, 16 (2007).
4. M. P. Kalashnikov, E. Risse, H. Schönnagel, and W. Sandner, Opt. Lett. pp. 923–925.
5. A. Jullien, O. Albert, F. Burgy, G. Hamoniaux, J.-P. Rousseau, J.-P. Chambaret, F. Augé-Rochereau, G. Chériaux, J. Etchepare, N. Minkovski, and S. M. Saltiel, Opt. Lett. pp. 920–922.
6. C. Dorrer, I. A. Begishev, A. V. Okishev, and J. D. Zuegel, Opt. Lett. pp. 2143–2145.
7. Y. Tang, I. Ross, C. Hernandez-Gomez, G. New, I. Musgrave, O. Chekhlov, P. Matousek, and J. Collier, Opt. Lett. **doc. ID 97340** (posted 5 September 2008, in press).
8. R. C. Shah, R. P. Johnson, T. Shimada, and B. M. Hegelich, sub. Eur. Phys. J. D (2008).
9. SNLO nonlinear optics code from A. V. Smith at `http://www.sandia.gov/imrl/X1118/xxtal.htm`.
10. A. Jullien, Ph.D. thesis, École Polytechnique (2006).
11. Z. Bör, B. Rácz, G. Szabó, M. Hilbert, and H. A. Hazim, Opt. Eng. p. 2501.
12. E. J. Divall and I. N. Ross, Opt. Lett. pp. 2273–2275.

13. R. P. Johnson *et al.* In prep. (2008).